A&A 406, 741–749 (2003)
DOI: 10.1051/0004-6361:20030660

Astronomy & Astrophysics

Trends in E2 and M1 transition rates between $3p_{3/2}$ and $3p_{1/2}$ levels in $3s^2\,3p^k$ systems

E. Charro, S. López-Ferrero, and I. Martín

Departamento de Química Física, Universidad de Valladolid, 47011 Valladolid, Spain

Received 23 December 2002 / Accepted 2 April 2003

Abstract. The analysis of forbidden lines, such as E2 and M1, in the atomic spectra emitted by certain ions is important for the study of the plasma in astrophysical objects and fusion devices. Transition rates between $3p_{3/2}$ and $3p_{1/2}$ levels in $3s^2\,3p^k$ ions that belong to the aluminium sequence have been calculated with the Relativistic Quantum Defect Orbital (RQDO) method. The present data are tested by comparison with other theoretical data available in the literature, and the regularity of the transition intensities along the isoelectronic sequence for both (E2 and M1) lines, as well as their competition, are also analysed.

Key words. atomic data – methods: numerical

1. Introduction

Within the last few years, the determination of atomic oscillator strengths and related properties for ionized systems has been an active research area on account of its considerable interest in astrophysics, plasma physics, laser physics and thermonuclear fusion research. In astrophysics, transitions from metastable levels of highly ionized atoms are observed in emission in low-density media. It is well known that line intensities and ratios provide excellent diagnostics for temperature and density and consequently for elemental abundances (Feldman 1981; Herter et al. 1982). In the laboratory, the np^k configurations of medium-Z elements have attracted considerable attention in recent years as spectroscopic diagnostics in Tokamak plasmas. This is due to the fact that they may give rise to strong lines at much longer wavelengths ($\lambda = 2000$ Å) than other transitions in the same ion. However, it is still difficult to measure accurately oscillator strengths, particularly for highly ionizad atoms where the available experimental techniques have limitations, and the reproduction in the laboratory of the very extreme conditions to which the constituents of the universe are subjected is extremely difficult.

Experimental transition rates for forbidden lines are scarce and, in most cases, missing when the degree of ionization is higher than 2. It is therefore necessary to rely upon theoretical values. One way to assess the quality of a given theoretical method is a comparison of the so-obtained results with some other measurable quantity which might be available (mostly the observed energies), and by comparison with the results supplied by other computers codes.

Send offprint requests to: E. Charro,
e-mail: lmnieto@wamba.cpd.uva.es

On the theoretical side, quantum-mechanical calculations have, thus, become crucial in the accomplishment of these goals. Wiese (1987) long pointed out the usefulness of procedures which account for relativistic effects, the mass production of data for complex atomic systems with increasingly refined semiempirical approaches; and the application of regularities among transition rates, such as the dependence on the nuclear charge, for the scaling of transition rates along isoelectronic sequeces or spectral series.

Many calculations have been done for the ions isoelectronic with Al, most of them corresponding to allowed transitions. In this context, we have reported oscillator strengths corresponding to dipole-allowed transitions for a group of Al-like ions ($Z = 13-103$) in a previous paper (Lavín et al. l997), in which the Relativistic Quantum Defect Orbital (RQDO) method, was employed. For forbidden transitions, no data have been reported with this method for this sequence before the present calculations.

Certain forbbiden transitions only become possible through the fine-structure splitting of an LS term into a series of J levels. Examples are the M1 and E2 transitions between the $3s^2 3p\ ^2P_{1/2}$ and $3s^2 3p\ ^2P_{3/2}$ levels in the aluminium sequence. In the non-relativistic approximation, these levels are degenerate. Calculations for the $3p\ ^2P_{3/2} \rightarrow 3p\ ^2P_{1/2}$ transition, corresponding to both E2 and M1 forbidden mechanisms, have presently been performed with the RQDO method, for the aluminium-like elements ranging from Sc IX ($Z = 21$) to Hg LXVIII ($Z = 80$). It is well known that fine-structure lines are interesting from a spectroscopic point of view, given their usefulness in spectral analysis in astrophysics and fusion plasma research.

The systematic trend of the A-values for E2 and M1 transitions along the isoelectronic sequence has also been analysed

in this work. In previous works (e.g., Lavín et al. l997) we studied the systematic trends of E1 spectral lines. The regular behaviour of oscillator strengths along isoelectronic sequences has proven to be a useful tool for analysing a large body of f-value data. It may also be exploited to obtain additional oscillator strengths by simple interpolation techniques (Martin & Wiese 1996).

Some theoretical E2 and M1 transition rates for aluminium-like elements are available in the literature. The most extensive group of data has been published by Huang (1986), who calculated transition rates for the ions comprised in the $13 \leq Z \leq 106$ range with the multiconfiguration Dirac-Fock (MCDF) technique.

In the present work, we deal with heavy ions and in high degree of ionization for which the relativistic contributions to the wavefunctions and energies of the levels involved in the transitions may not be negligible. We have consequently followed a theoretical method that gives explicit account of relativistic effects, the Relativistic Quantum Defect Orbital (RQDO) formalism, as mentioned above.

For over a decade, we have applied the RQDO method (Martín & Karwowski 1991; Karwowski & Martín 1991; Martín et al. 2000) to the calculation of atomic data in several isoelectronic sequences (see, e.g. Martín et al. 1993; Lavín et al. 1997; Charro & Martín 1998; Charro et al. 1996, 1997, 2000, 2001). The RQDO formalism, as opposed to sophisticated and costly self-consistent-field procedures, is a simple but reliable analytical method based on a model Hamiltonian. It has the great advantage that the computational effort is not increased for Z-high systems. The convenience of employing exactly solvable model potentials for calculating atomic transition rates manifests itself not only from a practical point of view but also because of the involved physical implications, when they are capable of achieving a good balance between computational effort and accuracy of results. In the present calculations, a general good accord between the RQDO transition probabilities and the comparative theoretical data is also found.

2. The RQDO method

The Relativistic Quantum Defect Orbital (RQDO) method has been described in detail in previous papers (Karwowski & Martín 1991; Martín et al. 2000). Therefore, we shall only briefly summarise its most fundamental aspects.

The relativistic formulation of the Quantum Defect Orbital (QDO) formalism, as developed by Martín & Karwowski (1991) and Karwowski & Martín (1991) was based on the decoupling of the Dirac second-order equation, and in the interpretation of the resulting solutions that had been carried out by Karwowski & Kobus (1985, 1986). These authors generalised the decoupling procedure of Biedenharn (1962) in such a way that it may be applied to the case of a general atomic spherical potential. They also showed that both the large and small components of the Dirac wavefunction may be recovered without any computational effort.

The quantum defect orbitals are solutions of the Schrödinger equation (Simons 1974; Martín & Simons 1975, 1976)

$$\left[-\frac{\mathrm{d}^2}{\mathrm{d}r^2} + \frac{\chi(\chi+1)}{r^2} - \frac{Z_{\mathrm{net}}}{r}\right]\psi_k{}^{\mathrm{QD}} = 2E^{\mathrm{QD}}\psi_k{}^{\mathrm{QD}}, \tag{1}$$

where Z_{net} is the nuclear charge on the active electron at large r and

$$\chi = n - \delta + c, \tag{2}$$

where δ is the quantum defect and c is an integer chosen to ensure the correct number of nodes and the normalization of the radial wave function. The eigenvalue E^{QD} in Eq. (1) depends only upon the nonintegral part of χ and, hence, is independent of c. The quantum defect is empirically obatained from the following equation:

$$E^{\mathrm{QD}} = E^x = -\frac{(Z_{\mathrm{net}})^2}{2(n-\delta)^2}, \tag{3}$$

where E^x is the experimental energy.

Analogously to the nonrelativistic case, Eq. (1), the RQDO equation is written as

$$\left[-\frac{\mathrm{d}^2}{\mathrm{d}r^2} + \frac{\Lambda(\Lambda+1)}{r^2} - \frac{2Z'_{\mathrm{net}}}{r}\right]\psi_k{}^{\mathrm{RD}} = 2e^{\mathrm{RD}}\psi_k{}^{\mathrm{RD}}, \tag{4}$$

with

$$Z'_{\mathrm{net}} = Z_{\mathrm{net}}\left(1 + \alpha^2 E^x\right), \tag{5}$$

and,

$$\Lambda = s - 1 - \delta' + c, \tag{6}$$

when $j = l + 1/2$, or

$$\Lambda = -s - \delta' + c, \tag{7}$$

when $j = l - 1/2$. δ' is the relativistic quantum defect, c is an integer with the same physical significance as that of Eq. (2); Z'_{net} is the scaled nuclear charge acting on the valence electrons at large radial distances; E^x is also here the experimentally measured energy. Atomic units are used throughout.

The relativistic quantum defect is determined empirically. We have

$$e^{\mathrm{RD}} = -\frac{(Z'_{\mathrm{net}})^2}{2(\eta-\delta')^2} \tag{8}$$

and is has been proven (Martín & Karwowski 1991) that the value of δ' may be obtained from:

$$-\frac{(Z_{\mathrm{net}})^2}{2(\eta-\delta')^2} = E^x\frac{(1+\alpha^2E^x/2)}{(1+\alpha^2E^x)^2}. \tag{9}$$

Here η is the relativistic principal quantum number, related with n, the principal quantum number, as follows

$$\eta = n - |k| + |s|. \tag{10}$$

It should be stressed that this formulation is "exact" in the sense that is equivalent to a four-component formulation based on the

standard first-order form of the Dirac equation. All matrix elements, in particular the transition moments, may be expressed in a simple way, using the solutions of the second-order equation. A set of recurrent formulas which are fulfilled by the radial integrals (Martín et al. 2000) allows the formalism to be very simple and compact. Karwowski & Martín (1991) have observed that the relativistic density distribution approximates very well the exact one at large values of r. At small distances, the quality of the density deteriorates, as happens when the nonrelativistic QDO densities are compared with the exact nonrelativistic ones (Simons 1974). Fortunately, the consequences of this drawback are very seldom reflected in the quality of the QDO and RQDO transition rates, because the strongest contribution to radial matrix elements comes, in most cases, from large radial distances.

The most important difference between the RQDO and QDO equations is the explicit dependence of the former on the total angular momentum quantum number k. As a consequence, values of the relativistic quantum defect are determined from the fine structure energies rather than from their centers of gravity. The corresponding relativistic quantum defect orbitals are different for each component of a multiplet and, if $c = 0$, they retain the nodal structure of the large components of the hydrogenic Dirac wave function.

The Relativistic Quantum Defect Orbital is expressed in terms of Kummer's functions,

$$\psi_k(r)^{\mathrm{RD}} = C\,\exp\left(\frac{-Z'_{\mathrm{net}}r}{\eta^*}\right)\left(\frac{2Z'_{\mathrm{net}}r}{\eta^*}\right)^{\Lambda+1} \times F\left(-(\eta^*-\Lambda-1), 2\Lambda+2, \frac{2Z'_{\mathrm{net}}r}{\eta^*}\right) \quad (11)$$

and C is the normalization constant,

$$C = \left(\frac{2Z'_{\mathrm{net}}}{\eta^*}\right)^{1/2}\left[\frac{\Gamma(\eta^*+\Lambda+1)}{2\eta^*\Gamma(\eta^*-\Lambda)}\right]^{1/2}\frac{1}{\Gamma(2\Lambda+2)} \quad (12)$$

with $\eta^* = \eta - \delta'$.

Since the effective Hamiltonian in Eq. (4) includes a screening term, the relativistic quantum defect orbitals are approximately valid in the core region of space. Core polarization effects are implicitly included in the calculations, as they are accounted for in the Λ parameter of the model Hamiltonian. On the other hand, given the one-electron nature of the RQDO formalism, it can be expected to perform better in highly excited states, where the active electron interacts less with the core and other valence electrons, than in low-lying energy states. The relativistic quantum defect orbitals lead to closed-form analytical expresions for the transition integrals. This allows one to calculate transition probabilities and oscillator strengths by simple algebra and with high computational costs/efficiency ratio.

3. Electric dipole forbidden transitions

The RQDO methodology supplies one-electron radial wavefunctions, characterized by the n, l and j quantum numbers (Martín & Karwowski 1991), that we employ in the transition matrix elements for the initial and final states of the active electron. These correspond to levels of a given L, S and J symmetry in many-electron atoms.

3.1. Transitions via electric quadrupole mechanism

Let us consider electric multipole radiation. The operator responsible for the interaction of this radiation with an atomic system is the electric multipole moment introduced by the general expression

$$Q_m^{(q)} = -\sum r_i^q C_m^{(q)}(i) \quad (13)$$

with

$$C_m^{(q)}(i) = \left(\frac{4\pi}{2q+1}\right)^{1/2} Y_{qm}(\theta_i,\varphi_i) \quad (14)$$

where $Y_{qm}(\theta_i,\varphi_i)$ are the spherical harmonics.

In the particular case of $q = 2$, the transitions take place via the electric quadrupole mechanism, E2. In this context, the electric quadrupole line strength for a transition between two states within the LSJ-coupling, which is the coupling scheme followed throughout in this work, in the notation of Condon & Shortley (1935), is given by the equation

$$S^{(2)}_{nlj,n'l'j'} = \frac{2}{3}\left|\left\langle \alpha J \parallel Q^{(2)} \parallel \alpha' J'\right\rangle\right|^2 \quad (15)$$

where α and α' are here the sets of quantum numbers which define the lower and upper states, respectively. The matrix-elements have the form

$$\langle \alpha J \parallel Q^{(2)} \parallel \alpha' J'\rangle = [(2J+1)(2J'+1)]^{1/2} \times W(SJL'2,LJ')\langle \alpha L \parallel Q^{(2)} \parallel \alpha' L'\rangle \delta_{SS'} \quad (16)$$

and the Kronecker delta, $\delta_{SS'}$, occurs because the electric multipole operators do not depend on spin. Thus, we define a line factor R_{line} by

$$R_{\mathrm{line}}(SLJ,S'L'J') = (2J+1)^{1/2}(2J'+1)^{1/2} \times W(SJL'2,LJ') \quad (17)$$

where $W(SJL'2,LJ')$ are the Racah coefficients which can be described in terms of $6j$-symbols

$$W(SJL'2,LJ') = (-1)^{S+J+L'+2}\begin{Bmatrix} S & J & L \\ 2 & L' & J' \end{Bmatrix}. \quad (18)$$

The line strength then becomes

$$\begin{aligned} S^{(2)}_{nlj,n'l'j'} &= \frac{2}{3}(2J+1)(2J'+1)\left[W(SJL'2,LJ')\right]^2 \\ &\quad \times \left|\left\langle \alpha L \parallel Q^{(2)} \parallel \alpha' L'\right\rangle\right|^2 \\ &= \frac{2}{3}\left[R_{\mathrm{line}}(SLJ,S'L'J')\right]^2 \\ &\quad \times \left|\left\langle \alpha L \parallel Q^{(2)} \parallel \alpha' L'\right\rangle\right|^2 . \end{aligned} \quad (19)$$

As mentioned above, the relevant operator is independent of spin, and hence spin does not change during the transition. The following selection rules apply to E2 transitions: $\Delta S = 0$, ΔL and $\Delta J = \pm 2, \pm 1, 0$, $L + L' \geq 2$, and $J + J' \geq 2$.

Thus, the reduced matrix element $\langle \alpha L \parallel Q^{(2)} \parallel \alpha' L' \rangle$ provides the relative strengths of different multiplets. We can write this reduced matrix element as the product of a single-electron reduced matrix element $\langle nl \parallel Q^{(2)} \parallel n'l' \rangle$, which depends on only the quantum numbers of the jumping electron, and a factor that we shall call the multiplet factor, $R_{\rm mult}$:

$$\langle \alpha L \parallel Q^{(2)} \parallel \alpha' L' \rangle = R_{\rm mult}(\alpha L, \alpha' L) \times \langle nl \parallel Q^{(2)} \parallel n'l' \rangle \quad (20)$$

where

$$\langle nl \parallel Q^{(2)} \parallel n'l' \rangle = \langle l \parallel C^{(2)} \parallel l' \rangle \langle R_{nlj} | Q^{(2)} | R_{n'l'j'} \rangle \quad (21)$$

in Eq. (21), $\langle R_{nlj} | Q^{(2)} | R_{n'l'j'} \rangle$ is the radial transition integral, $\langle l \parallel C^{(2)} \parallel l' \rangle$ is the pertinent reduced matrix element, which can be evaluated using $3j$-symbols by the following expresion

$$\langle l \parallel C^{(2)} \parallel l' \rangle = [l, l'] \begin{pmatrix} l & 2 & l' \\ 0 & 0 & 0 \end{pmatrix} \quad (22)$$

and $R_{\rm mult}$ may be expressed as follows:

$$R_{\rm mult}(\alpha L, \alpha' L') = (2L+1)^{1/2} (2L'+1)^{1/2} W(L_{\rm c} L l' 2, l L') \quad (23)$$

where $L_{\rm c}$ refers to the orbital angular momentum of the atomic core, and the last symbol in Eq. (23) is,

$$W(L_{\rm c} L l' 2, l L') = (-1)^{L_{\rm c}+L+l'+2} \begin{Bmatrix} L_{\rm c} & L & l \\ 2 & l' & L' \end{Bmatrix}. \quad (24)$$

Finally, the line strength takes the form

$$S^{(2)}_{nlj,n'l'j'} = \frac{2}{3} \mid R_{\rm line}(S L J, S' L' J') R_{\rm mult}(\alpha L, \alpha' L') \times \langle L \parallel C^{(2)} \parallel L' \rangle \langle R_{nlj} | Q^{(2)} | R_{n'l'j'} \rangle \mid^2 . \quad (25)$$

The total strength of the line strengths of all the lines in a multiplet is therefore:

$$S(\gamma L, \gamma' L') = \sum_{JJ'} S(\gamma J, \gamma' J'). \quad (26)$$

Thus, the line strength for a multiplet transition is

$$S(\gamma L, \gamma' L') = (2S+1) \mid \langle \alpha L \parallel Q^{(2)} \parallel \alpha' L' \rangle \mid^2 = (2S+1) \mid R_{\rm mult}(\alpha L, \alpha' L') \langle nl \parallel Q^{(2)} \parallel n'l' \rangle \mid^2 . \quad (27)$$

The relationships between the line strength $S^{(2)}$ (in atomic units, $e^2 a_0^4$), the oscillator strength $f^{(2)}$ (dimensionless), and the transition rate $A^{(2)}$ (in s^{-1}) for E2 transitions are given by (Sobelman 1979)

$$g' A^{(2)} = (8\pi^2 \hbar \alpha / m \lambda^2) g f^{(2)} = (6.6703 \times 10^{15} / \lambda^2) g f^{(2)} \quad (28)$$

$$g' A^{(2)} = (32\pi^5 \alpha c a_0^4 / 15 \lambda^5) S^{(2)} = (1.11995 \times 10^{18} / \lambda^5) S^{(2)} \quad (29)$$

where λ is the transition wavelength (in Å), g and g' are the degeneracies of the lower and upper state, respectively, and α is again the fine-structure constant.

3.2. Transitions via magnetic dipole mechanism

Let us consider now the magnetic multipole radiation. The operator responsible for the interacton of this radiation with matter is the magnetic multipole moment introduced by the general expression

$$\mathcal{M}^{(q)}_m = \sum_i r_i^{q-1} \sqrt{q(2q-1)} \left\{ \frac{1}{q+1} \left[C^{(q-1)}_m \times l^1_i \right]^q + \left[C^{(q-1)}_m (i) \times s^1_i \right]^q_m \right\}. \quad (30)$$

In the particular case of $q = 1$, when the transitions are taking place via the magnetic dipole mechanism, M1,

$$\mathcal{M}^{(1)}_m = \sum_i \frac{1}{2} \left[l^1_i + 2 s^1_i \right] \quad (31)$$

where l^1 and s^1 are vector operators of orbital and spin momenta.

In this context, the formulae for the probability of magnetic dipole (M1) transitions do not contain radial integrals, an thus, the line strength, $S^{\rm M1}$, is independent of the frequency of the transition.

The magnetic dipole line strength for a transition between two states within the LSJ-coupling, in the notation of Condon & Shortley (1935), is given by the equation

$$S^{\rm (M1)}_{nlj,n'l'j'} = |\langle \alpha J \parallel \mathcal{M}^{(1)} \parallel \alpha' J' \rangle|^2. \quad (32)$$

The final expression is

$$S^{\rm M1}(LJ, LJ-1) = \frac{1}{4J} \left(L + \frac{1}{2} + J + 1 \right) \times \left(L + \frac{1}{2} - J + 1 \right) \left(\frac{1}{2} + J - L \right) \left(J + L - \frac{1}{2} \right). \quad (33)$$

The transition rate $A^{\rm M1}$ (in s^{-1}) is related with the line strength $S^{\rm M1}$, in Bohr magneton units ${\mu_{\rm B}}^2$, by the expression

$$A^{M1} = (2.697\, 10^{13} / \lambda^3) \frac{S^{\rm M1}}{g'}. \quad (34)$$

The relationship between the oscillator strength $f^{\rm M1}$ (dimensionless) and the transition rate $A^{\rm M1}$ (in s^{-1}) is given by Eq. (28), which is generally valid for E1, E2 and M1 transitions.

4. Regularities along the isoelectronic sequence

Regularities in individual oscillator strengths along an isoelectronic sequence as functions of the nuclear charge have been predicted for E1 transitions from conventional perturbation theory (Cohen & Dalgarno 1966; Dalgarno & Parkinson 1967). We shall now extend this procedure to the analysis of electric quadrupole transitions.

If we denote the generalised radial transition integral

$$|\langle R_{nlj} | r^q | R_{n'l'j'} \rangle| = I^{(q)}_{nlj,n'l'j'}, \quad (35)$$

for a given operator, the variation of a matrix element as a function of Z may be studied by the Rayleigh-Schrödinger perturbation theory. If we introduce $\rho = Z.r$ and $\epsilon = EZ^{-2}$ in a.u., the expansions of ψ and E in powers of the perturbation parameter, Z^{-1}, are:

$$\psi_{nlj,n'l'j'} = \psi_0 + \psi_1.Z^{-1} + \psi_2.Z^{-2} + ... \quad (36)$$

and

$$E = Z^2(\epsilon_0 + \epsilon_1.Z^{-1} + \epsilon_2.Z^{-2} + ...). \quad (37)$$

The electric dipole ($q = 1$) transition integral is given by the following Z-expansion:

$$|\langle\psi_{nlj}|\rho|\psi_{n'l'j'}\rangle| = I^{(1)}_{nlj,n'l'j'} = I^{(1)}_0.Z^{-1} + I^{(1)}_1.Z^{-2} + ... \quad (38)$$

where I_0 is the corresponding integral for hydrogen and the superscript (1) refers to E1 or electric dipole transitions.

The dipole line strength, or squared radial integral Eq. (38), may be written as:

$$S^{(1)}_{nlj,n'l'j'} = S^{(1)}_0.Z^{-2} + S^{(1)}_1.Z^{-3} + S^{(1)}_2.Z^{-4} + ... \quad (39)$$

and the expression for the E1 oscillator strength will be

$$f^{(1)}_{nlj,n'l'j'} = f^{(1)}_0 + f^{(1)}_1.Z^{-1} + f^{(1)}_2.Z^{-2} + ... \quad (40)$$

For the line and oscillator strengths, as well as for the transition rate A, it is possible to perform paralell nuclear charge expansion representations in the quadrupole case to study systematic trends of E2 S- or f-values along an isoelectronic sequence. Here the transition operator, ρ^2, leads to (Biémont & Godefroid 1978),

$$S^{(2)}_{nlj,n'l'j'} = S^{(2)}_0.Z^{-4} + S^{(2)}_1.Z^{-5} + S^{(2)}_2.Z^{-6} + ... \quad (41)$$

with

$$S^{(2)}_0 = |<\psi_{nlj}|\rho^2|\psi_{n'l'j'}>|^2. \quad (42)$$

For the transition rate A, the corresponding expansion is the following,

$$A^{(2)}_{n'l'j',nlj} = A^{(2)}_0.Z^6 + A^{(2)}_1.Z^5 + A^{(2)}_2.Z^4 + A^{(2)}_3.Z^3 + ..., \quad (43)$$

and the quadrupole oscillator strength may be written, as,

$$f^{(2)}_{nlj,n'l'j'} = f^{(2)}_0.Z^2 + f^{(2)}_1.Z + f^{(2)}_2 + f^{(2)}_3.Z^{-1} + ..., \quad (44)$$

where $f^{(2)}_0$, $f^{(2)}_1$, $f^{(2)}_2$, ... are proportional to some power of $\Delta\epsilon_0$, the hydrogenic transition energy corresponding to the transition under study. We may also consider of interest to analyze the behaviour of $f^{(2)}.Z^{-2}$ along the isoelectronic sequence. From Eq. (44) it is inferred:

$$f^{(2)}_{nlj,n'l'j'}.Z^{-2} = f^{(2)}_0 + f^{(2)}_1.Z^{-1} + f^{(2)}_2.Z^{-2} + ... \quad (45)$$

When no change of the principal quantum number occurs ($\triangle n = 0$) during the transition, if we ignore relativistic effects, $\triangle\epsilon_0 = 0$. We have thus:

$$f^{(2)}_{lj,l'j'} = f^{(2)}_3.Z^{-1} + f^{(2)}_4.Z^{-2} + ... \quad (46)$$

That is, the curve of $f^{(2)}$ versus Z^{-1} would tend to an asymptotic zero value in the high-Z side of the sequence if no relativistic effects were present. Equation (45) is expected to be a good approximation to the behaviour of the oscillator strength with Z^{-1} for E2 transitions at least for the first few ions of the sequence of a light element, e.g., Na I, where relativistic effects still are not very important. However, as soon as these effects set in, deviations from Eq. (45), as well as from all the expressions in this section, are expected to occur.

5. Energy data

5.1. Energy levels

In the RQDO context, the quantum defects are often extracted from energy level data. As energy levels, we have employed those provided from the critical compilation by Kelly (1987). These data comprise the elements from Al I to Kr XXIV. Given that the transitions we can study are constrained by the availability of observed energy levels, for the ions for which no data were found, interpolated (e.g. Br XXIII) and extrapolated ($37 \leq Z \leq 80$) energy values have been used. In order to do this, we first fitted the experimental energy data (belonging to ions between $Z = 13$ and $Z = 36$, with the exception of the value for $Z = 35$) to a polynomic dependence of the nuclear charge, Z. The expression obtained for the $3p\,^2P_{3/2}$ level is,

$$E_{3p_{3/2}} = 0.136551\,Z^4 - 4.32196\,Z^3 + 72.6444\,Z^2 - 779.776Z + 3577.09 \quad (47)$$

where E is in cm^{-1} and the correlation factor was found to be 0.9999.

As we advance in the sequence, a Z-value will be reached for which the spin-orbit coupling scheme can no longer be expected be pure LSJ scheme but an intermediate one between that and jj. We have not changed, however, the formulation of either the radial functions or the angular factors employed in the calculation of oscillator strengths at any point in the sequence. We expect that the use of emppirical energy data will, at least to some extent, account for intermediate coupling, as it does, at all values of Z, for configuration interaction.

5.2. Ionization energy

Other input data also needed in the RQDO calculations are the ionization energies of the atomic systems. The corresponding values from Al I to Kr XXIV have been taken from Kelly (1987). Analogously to the energy levels, a fitting of the experimental data (with the exception of Br XXIII) has led to the following expression for the ionization energy in terms of powers of Z

$$I.E. = -2.07672 - 369447\,Z + 17639.8\,Z^2 - 70.2101\,Z^3 \quad (48)$$

where $I.E.$ is given in cm^{-1}, an the correlation factor was equal to 0.9999. With this formula, the gap of values for $I.E.$ can be interpolated ($Z = 35$) and extrapolated ($37 \leq Z \leq 80$).

6. Analysis of the results

In Table 1, the wavelengths corresponding to the $3p\ ^2P_{3/2} \rightarrow 3p\ ^2P_{1/2}$ spectral line for a large number of Al-like ions are

Table 1. Wavelenght (λ in Å) for the $3p_{1/2} - 3p_{3/2}$ spectral line in the aluminium sequence.

Z	λ^a	λ^b	Z	λ^a	λ^b
21	17369.592	17095.820	51	198.848	196.825
22	13266.334	13140.749	52	181.887	179.708
23	10320.540	10266.303	53	166.691	164.373
24	8161.484	8137.911	54	153.045	150.604
25	6542.527	6534.657	55	140.762	138.212
26	5308.476	5308.261	56	129.684	127.038
27	4353.431	4357.040	57	119.672	116.942
28	3604.572	3609.913	58	110.604	107.802
29	3005.676	3016.376	59	102.377	99.512
30	2534.457	2539.926	60	94.899	91.981
31	2148.857	2153.855	61	88.089	85.127
32	1833.956	1838.301	62	81.878	78.879
33	1574.163	1578.329	63	76.204	73.174
34	1358.880	1362.578	64	71.011	67.958
35	1179.739	1182.312	65	66.252	63.182
36	1027.708	1030.743	66	61.884	58.802
37	900.103	902.559	67	57.869	54.780
38	791.571	793.567	68	54.174	51.081
39	698.865	700.411	69	50.769	47.677
40	619.301	620.415	70	47.626	44.538
41	550.707	551.411	71	44.723	41.642
42	491.321	491.646	72	42.036	38.966
43	439.703	439.671	73	39.548	36.491
44	394.666	394.303	74	37.241	34.199
45	355.231	354.561	75	35.110	32.074
46	320.585	319.633	76	33.110	30.103
47	290.047	288.838	77	31.258	28.272
48	263.049	261.606	78	29.535	26.570
49	239.110	237.454	79	27.461	24.986
50	217.824	215.975	80	26.428	23.511

[a] This work.

[b] Huang 1986.

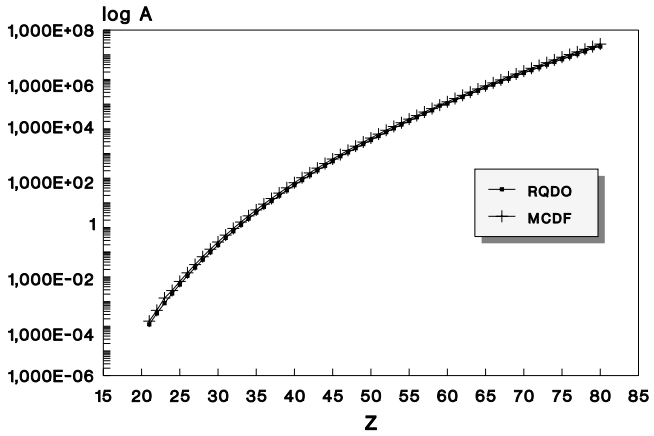

Fig. 1. Systematic trends of the transition rates for the 3p $^2P_{3/2}$–3p $^2P_{1/2}$ spectral line via the electric quadrupole (E2) mechanism along the aluminium sequence.

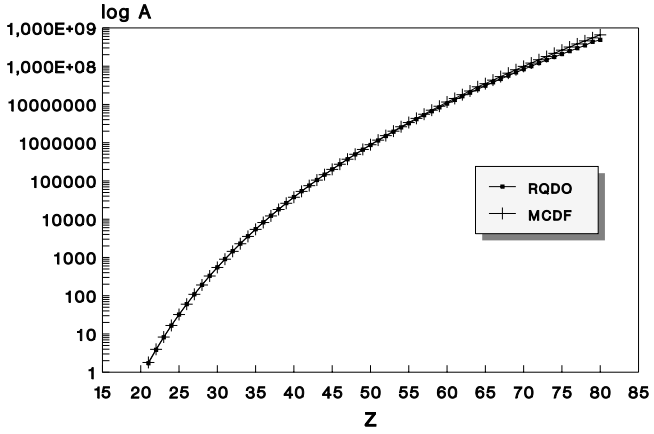

Fig. 2. Systematic trends of the transition rates for the 3p $^2P_{3/2}$–3p $^2P_{1/2}$ spectral line via the magnetic dipole (M1) mechanism along the aluminium sequence.

collected. The data employed in the present calculations are compared with those reported by Huang (1986). In Table 2, the presently calculated oscillator strengths are compared with those reported by Huang (1986), which are, to our knowledge, the only data existing in the literature, as regards these transitions and atomic systems. No experimental results have been found.

The values supplied by Huang (1986), have been calculated with the multiconfiguration Dirac-Fock (MCDF) computer code of Desclaux (1975), which includes contributions from the Breit interaction, as well as those from the Lamb shifts. Huang included all the configurations that arise from within the $n = 3$ complex in his calculations.

The E2 and M1 f-values collected in Table 2, comprise the ions from Sc IX ($Z = 21$) up to Hg LXVIII ($Z = 80$). The magnetic dipole the line strength has been taken as $1.3333\,\mu_B^2$ according to Eq. (33).

The main contribution to the intensity of the spectral line can be analysed by comparing the f-values corresponding to the M1 and E2 transitions for each ion of the sequence. The contribution of the E2 transition turns out to be negligible with respect to that of the M1 transition, the latter being several orders of magnitude larger than the former. An inspection of Table 2 reveals a rather good general agreeement between our results and those reported by Huang (1986).

Additionally, in Figs. 1 and 2, the behaviour of the E2 and M1 transition probabilities, respectively, along the isoelectronic sequence is analysed in graph form. The value of Log A has been plotted against the atomic number, Z, from $Z = 21$ up to $Z = 80$. The MCDF (Huang 1986) data have also been included. These figures serve two purposes. One is to show the agreement or deviations between our results and the MCDF calcuations. The second is to reflect the systematic trends complied with by the individual RQDO A-values along the isoelectronic sequence, which have long been considered

Table 2. E2 and M1 oscillator strengths for the $3p_{1/2} - 3p_{3/2}$ spectral line.

ION	Z	$f(E2)^a$	$f(E2)^b$	$f(M1)^a$	$f(M1)^b$
Sc IX	21	1.072(−11)	1.412(−11)	1.548(−07)	1.576(−07)
Ti X	22	1.751(−11)	2.283(−11)	2.027(−07)	2.050(−07)
V XI	23	2.748(−11)	3.599(−11)	2.605(−07)	2.624(−07)
Cr XII	24	4.225(−11)	5.542(−11)	3.249(−07)	3.310(−07)
Mn XIII	25	6.311(−11)	8.353(−11)	4.109(−07)	4.121(−07)
Fe XIV	26	9.370(−11)	1.235(−10)	5.065(−07)	5.073(−07)
Co XV	27	1.356(−10)	1.792(−10)	6.176(−07)	6.179(−07)
Ni XVI	28	1.937(−10)	2.560(−10)	7.459(−07)	7.457(−07)
Cu XVII	29	2.706(−10)	3.601(−10)	8.945(−07)	8.922(−07)
Zn XVIII	30	3.727(−10)	4.998(−10)	1.061(−06)	1.059(−06)
Ga XIX	31	5.268(−10)	6.849(−10)	1.251(−06)	1.249(−06)
Ge XX	32	7.115(−10)	9.278(−10)	1.466(−06)	1.463(−06)
As XXI	33	9.568(−10)	1.243(−09)	1.708(−06)	1.704(−06)
Se XXII	34	1.267(−09)	1.650(−09)	1.979(−06)	1.973(−06)
Br XXIII	35	1.670(−09)	2.168(−09)	2.279(−06)	2.273(−06)
Kr XXIV	36	2.185(−09)	2.826(−09)	2.616(−06)	2.607(−06)
Rb XXV	37	2.847(−09)	3.653(−09)	2.987(−06)	2.976(−06)
Sr XXVI	38	3.672(−09)	4.686(−09)	3.397(−06)	3.384(−06)
Y XXVII	39	4.705(−09)	5.968(−09)	3.847(−06)	3.832(−06)
Zr XXVIII	40	5.988(−09)	7.552(−09)	4.341(−06)	4.325(−06)
Nb XXIX	41	7.575(−09)	9.495(−09)	4.882(−06)	4.864(−06)
Mo XXX	42	9.527(−09)	1.187(−08)	5.472(−06)	5.453(−06)
Tc XXXI	43	1.192(−08)	1.475(−08)	6.115(−06)	6.095(−06)
Ru XXXII	44	1.483(−08)	1.823(−08)	6.812(−06)	6.793(−06)
Rh XXXIII	45	1.836(−08)	2.243(−08)	7.569(−06)	7.551(−06)
Pd XXXIV	46	2.262(−08)	2.745(−08)	8.387(−06)	8.372(−06)
Ag XXXV	47	2.775(−08)	3.345(−08)	9.270(−06)	9.260(−06)
Cd XXXVI	48	3.389(−08)	4.058(−08)	1.022(−05)	1.022(−05)
In XXXVII	49	4.123(−08)	4.903(−08)	1.124(−05)	1.125(−05)
Sn XXXVIII	50	4.995(−08)	5.901(−08)	1.234(−05)	1.236(−05)
Sb XXXIX	51	6.029(−08)	7.075(−08)	1.352(−05)	1.356(−05)

In this and the remaining tables, AE(B) denotes $A \times 10^B$.

as a qualitative proof of correctness (Wiese & Kelleher 1998) and can be used for the interpolation or extrapolation of non-calculated data.

In Fig. 3, we show only the present RQDO data in order to show the competition between both mechanism (E2 and M1) for the same transition.

6.1. Regularities in homologous series

Regularities in individual oscillator strengths along an isoelectronic sequence as functions of the nuclear charge have long been predicted from conventional perturbation theory (Cohen & Dalgarno 1966; Dalgarno & Parkinson 1967), and their usefulness in analysing the f-values has been repeatedly stressed (see, e.g., Martin & Wiese 1996 and references therein).

The oscillator strengths or transition rates for strong analogous ($nl \rightarrow n'l'$) transitions of homologous atoms are expected to be similar on account of the analogous outer electron structure of such elements. Thus, all alkali elements, for example, would be expected to exhibit similar f-values for the leading lines in a Rydberg series, and it is, indeed, well known that the principal resonance lines for the alkalis have f-values close to unity. However, one has to consider that as the elements within a chemical family become heavier, the outer atomic structure becomes modified due to the presence of unfilled electron shells. Generally, the systematic behaviour for homologous atoms is not expected to be as closely adhered to as for the case of a given transition along an isoelectronic sequence, where the electron configuration remains the same and only a scaling of the nuclear charge occurs, but it is observed in some cases. As an illustration, Figs. 4 and 5 display the behaviour of the transition rate for the $n\mathrm{p}\ ^2\mathrm{P}_{3/2} \rightarrow n\mathrm{p}\ ^2\mathrm{P}_{1/2}$ spectral line for two sequences, those of aluminium ($n = 2$) and Boron ($n = 3$) against ξ. ξ is defined as the charge of the atomic core

Table 2. continued.

ION	Z	f(E2)[a]	f(E2)[b]	f(M1)[a]	f(M1)[b]
TeXL	52	7.250(−08)	8.452(−08)	1.478(−05)	1.484(−05)
I XLI	53	8.689(−08)	1.006(−07)	1.613(−05)	1.621(−05)
Xe XLII	54	1.038(−07)	1.194(−07)	1.757(−05)	1.768(−05)
Cs XLIII	55	1.236(−07)	1.412(−07)	1.910(−05)	1.925(−05)
Ba XLIV	56	1.467(−07)	1.665(−07)	2.073(−05)	2.093(−05)
La XLV	57	1.736(−07)	1.958(−07)	2.247(−05)	2.271(−05)
Ce XLVI	58	2.049(−07)	2.296(−07)	2.431(−05)	2.462(−05)
Pr XLVII	59	2.411(−07)	2.685(−07)	2.626(−05)	2.664(−05)
Nd XLVIII	60	2.830(−07)	3.132(−07)	2.833(−05)	2.880(−05)
Pm XLIX	61	3.313(−07)	3.644(−07)	3.052(−05)	3.109(−05)
Sm L	62	3.870(−07)	4.229(−07)	3.284(−05)	3.351(−05)
Eu LI	63	4.508(−07)	4.898(−07)	3.528(−05)	3.609(−05)
Gd LII	64	5.241(−07)	5.660(−07)	3.786(−05)	3.881(−05)
Tb LIII	65	6.079(−07)	6.526(−07)	4.058(−05)	4.170(−05)
Dy LIV	66	7.035(−07)	7.509(−07)	4.345(−05)	4.475(−05)
Ho LV	67	8.123(−07)	8.623(−07)	4.646(−05)	4.797(−05)
Er LVI	68	9.366(−07)	9.884(−07)	4.963(−05)	5.138(−05)
Tm LVII	69	1.077(−06)	1.131(−06)	5.296(−05)	5.497(−05)
Yb LVIII	70	1.237(−06)	1.292(−06)	5.645(−05)	5.876(−05)
Lu LIX	71	1.418(−06)	1.473(−06)	6.012(−05)	6.275(−05)
Hf LX	72	1.622(−06)	1.676(−06)	6.396(−05)	6.696(−05)
Ta LXI	73	1.853(−06)	1.905(−06)	6.798(−05)	7.138(−05)
W LXII	74	2.113(−06)	2.161(−06)	7.219(−05)	7.603(−05)
Re LXIII	75	2.403(−06)	2.449(−06)	7.658(−05)	8.092(−05)
Os LXIV	76	2.734(−06)	2.760(−06)	8.120(−05)	8.606(−05)
Ir LXV	77	3.102(−06)	3.130(−06)	8.601(−05)	9.146(−05)
Pt LXVI	78	3.515(−06)	3.532(−06)	9.103(−05)	9.712(−05)
Au LXVII	79	4.190(−06)	3.979(−06)	9.790(−05)	1.031(−04)
Hg LXVIII	80	4.494(−06)	4.479(−06)	1.017(−04)	1.043(−04)

[a] This work.

[b] Huang (1986).

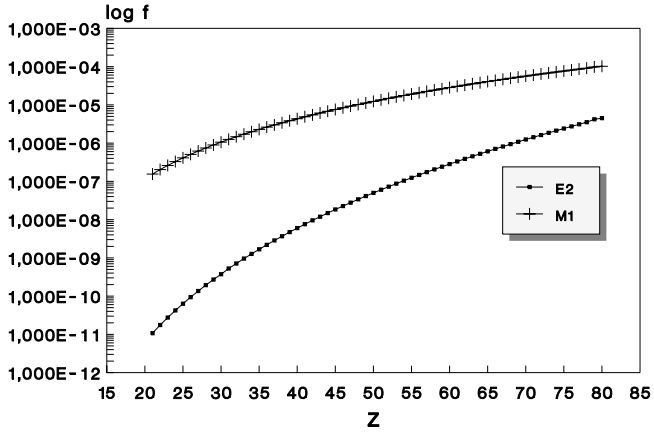

Fig. 3. Competition between the electric quadrupole (E2) and the magnetic dipole (M1) mechanism in the $3p\ ^2P_{3/2}$–$3p\ ^2P_{1/2}$ transition along the aluminium sequence.

($\xi = Z - N$), where Z is the nuclear charge and N is the number of core electrons. In this way, following the spectroscopic notation, for a neutral atom we have $\xi = 1$. The values for the transition rates via the magnetic dipole (M1) mechanism are shown in Fig. 4, and for the transition via the quadrupole (E2) mechanism in Fig. 5. The RQDO A-values plotted for B-like ions have been taken from Charro et al. (2001).

7. Conclusions

The RQDO procedure has once more proved to be a very useful tool for estimating transition rates and oscillator strengths. In the particular case of the Al-like ions, a general, satisfying, agreement is found between the RQDO results and those obtained with the rather more elaborate MCDF procedure which accounts for a great deal of electron correlation (Huang 1986).

Finally, the RQDO *A*-values for the E2 and M1 transitions follow the expected systematic trends along the isoelectronic sequence, which have long been considered as a qualitative proof of correctness and can be exploited for the interpolation or extrapolation of non-calculated data. We are confident in that

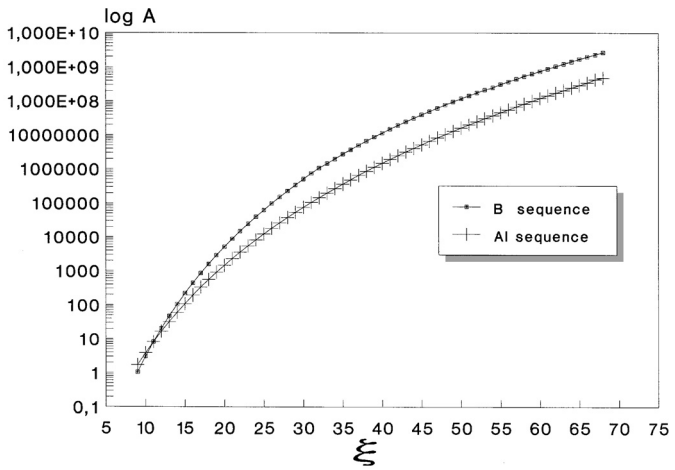

Fig. 4. Systematic trends for the fine-structure $3p\ ^2P_{3/2}$–$3p\ ^2P_{1/2}$ spectral line of the aluminium and boron sequences ($n = 3$ and 2, respectively). For both sequences, our RQDO transition rates via the magnetic dipole (M1) mechanism are plotted versus ξ, the charge on the atomic core or effective nuclear charge.

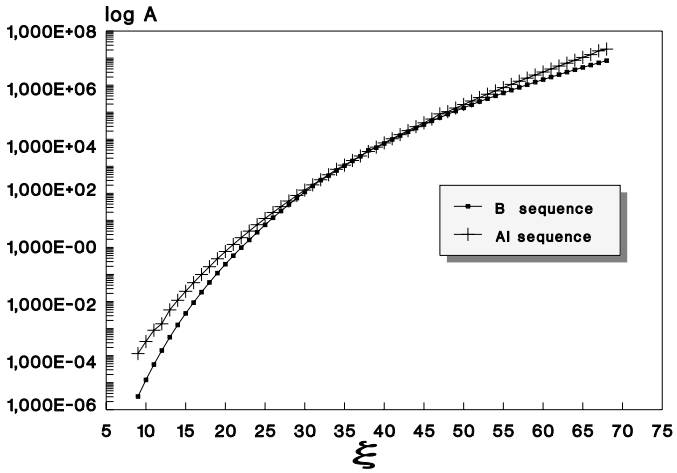

Fig. 5. Systematic trends for the fine-structure $3p\ ^2P_{3/2}$–$3p\ ^2P_{1/2}$ spectral line of the aluminium and boron sequences ($n = 3$ and 2, respectively). For both sequences, our RQDO transition rates via the electric quadrupole (E2) mechanism are plotted versus ξ, the charge on the atomic core or effective nuclear charge.

the present RQDO f-values, may be potentially useful in astrophysics and fusion plasma research.

Acknowledgements. This work has been supported by the DGI of the Ministry of Science and Technology within Project No. BQU2001-2935-CO2-O2 and the J.C.L. within Project No. VA119/02.

References

Biedenharn L. C. 1962, Phys. Rev., 126, 845
Biémont, E., & Godefroid, M. 1978, Phys. Scr. , 18, 323
Charro, E., & Martín, I. 1998, A&AS, 131, 523
Charro, E., Martín, I., & Lavín, C. 1996, J. Quant. Spectrosc. Radiat. Transfer, 56, 241
Charro, E., Martín, I., & Lavín, C. 1997, A&AS, 124, 397
Charro, E., Martín, I., & Serna, M. A. 2000 J. Phys. B., 33, 1753
Charro, E., López-Ferrero, S., & Martín, I. 2001, J. Phys. B., 34, 4243
Feldman, U. 1981, Phys. Scr., 24, 681
Cohen, M., & Dalgarno, A. 1966, Proc. Roy. Soc. (London), A293, 359
Condon, E. U., & Shortley, G. H. 1935, The Theory of Atomic Spectra (Cambridge, England: Cambridge University Press)
Dalgarno, A., & Parkinson, E. M. 1967, Proc. Roy. Soc. (London), A301, 253
Desclaux, J. P. 1975, Comput. Phys. Commun., 9, 31
Herter, T., Briotta, D. A., Gull G. E., Shure, M. A., & Houck, J. R. 1982, ApJ, 262, 164
Huang, K.-N. 1986, At. Data Nuclear Data Tables, 34, 1
Karwowski, J., & Kobus, J. 1985, Int. J. Quant. Chem., 28, 741
Karwowski, J., & Kobus, J. 1986, Int. J. Quant. Chem., 30, 809
Karwowski, J., & Martín, I. 1991, Phys. Rev., A, 43, 4832
Kelly, R. L. 1987, J. Chem. Ref. Data, 16, 1
Lavín, C., Alvarez, A. B., & Martín, I. 1997, J. Quant. Spectrosc. Radiat. Transfer, 57, 831
Martín, I., & Karwowski, J. 1991, J. Phys. B., 24, 1538
Martín, I., Karwowski, J., & Bielinska-Waz, D. 2000, J. Phys. A., 33, 823
Martín, I., Karwowski, J., Diercksen, G. H. F., & Barrientos, C. 1993, A&AS, 100, 595
Martín, I., & Simons, G. 1975, J. Chem. Phys., 62, 4799
Martín, I., & Simons, G. 1976, Mol. Phys., 32, 1017
Martin, W. C., & Wiese, W. L. 1996, in Atomic, Molecular, and Optical Physics Handbook American Institut of Physics, ed. G. W. F. Drake (New York: Woodbury), 135
Simons, G. 1974, J. Chem. Phys., 60, 645
Sobelman, I. I. 1979, Atomic Spectra and Radiative Transitions (Springer-Verlag)
Wiese, W. L. 1987, Phys. Scr., 35, 846
Wiese, W. L., & Kelleher, D. E. 1998, Atomic and Molecular Data and Their Applications, NIST Special Publication 926, ed. P. J. Mohr, & W. L. Wiese (Washington, DC: US Govt Printing Office), 105